

# Molecular orbital excitations in cuprates

Young-June Kim, J. P. Hill, and G. D. Gu

*Department of Physics, Brookhaven National Laboratory, Upton, New York 11973*

F. C. Chou

*Center for Materials Science and Engineering, Massachusetts Institute of Technology, Cambridge, Massachusetts 02139*

S. Wakimoto and R. J. Birgeneau

*Department of Physics, University of Toronto, Toronto, Ontario M5S 1A7, Canada*

Seiki Komiya and Yoichi Ando

*Central Research Institute of Electric Power Industry, Komae, Tokyo 201-8511, Japan*

N. Motoyama, K. M. Kojima, and S. Uchida

*Graduate School of Frontier Sciences, University of Tokyo, Bunkyo, Tokyo 113-8656, Japan*

D. Casa and T. Gog

*CMC-CAT, Advanced Photon Source, Argonne National Laboratory, Argonne, Illinois 60439*

(Dated: February 2, 2008)

We report resonant inelastic x-ray scattering studies of electronic excitations in a wide variety of cuprate compounds. Specifically, we focus on the charge-transfer type excitation of an electron from a bonding molecular orbital to an antibonding molecular orbital in a copper oxygen plaquette. Both the excitation energy and the amount of dispersion are found to increase significantly as the copper oxygen bond-length is reduced. We also find that the estimated bond-length dependence of the hopping integral  $t_{pd}$  is much stronger than that expected from tight-binding theory.

PACS numbers: 74.25.Jb, 74.72.-h, 78.70.Ck, 71.27.+a

## I. INTRODUCTION

One of the most important characteristics of the electronic structure of the cuprates is the strong hybridization between the Cu  $3d_{x^2-y^2}$  level and the O  $2p_\sigma$  level, where  $p_\sigma$  denotes the  $p_x$  or  $p_y$  orbitals pointing towards the Cu ions. Because of this hybridization, the Cu-O bond has a strong covalent character and a large energy splitting exists between the bonding ( $\sigma$ ) and antibonding ( $\sigma^*$ ) molecular orbitals. In the ionic limit without hybridization, this energy splitting corresponds to the energy difference between the atomic  $d_{x^2-y^2}$  and  $p_\sigma$  orbitals, which is  $\Delta_0 \sim 3.5$  eV.<sup>1</sup> As the  $p-d$  hybridization becomes larger, the energy splitting ( $\Delta_{\sigma\sigma^*}$ ) between the two molecular orbitals increases, reflecting the increasingly covalent nature of the Cu-O bonding. Thus,  $\Delta_{\sigma\sigma^*}$  is a direct measure of the Cu-O hybridization, and could serve as an independent route to determine the value of the hopping matrix element,  $t_{pd}$ , since it is believed that  $\Delta_{\sigma\sigma^*}$  is directly related to  $t_{pd}$ .<sup>2</sup> Although there has been no systematic theoretical study of  $\Delta_{\sigma\sigma^*}$ , the values obtained from first-principles calculations range widely from  $\sim 4$  eV to  $\sim 9$  eV.<sup>3,4,5,6</sup> For example, Martin and Hay<sup>5</sup> have carried out an *ab initio* quantum chemistry calculation of a cluster of copper oxygen octahedra ( $\text{CuO}_6^{10-}$ ) in  $\text{La}_{1.85}\text{Sr}_{0.15}\text{CuO}_4$ , and obtained  $\Delta_{\sigma\sigma^*} \sim 9$  eV, while in a recent density-functional calculation of a similar cluster, Hüsser and coworkers reported a value of  $\Delta_{\sigma\sigma^*} \sim 5.8$  eV.<sup>6</sup> Experimentally, determining this quan-

tity has been very difficult, since in this energy range transitions involving the La  $4f$  bands dominate the spectral features of optical spectroscopy.<sup>7</sup>

In this paper, we report a systematic experimental study of  $\Delta_{\sigma\sigma^*}$ , the excitation energy from bonding to antibonding molecular orbitals, using the recently developed resonant inelastic x-ray scattering (RIXS) technique.<sup>8,9</sup> RIXS is ideally suited for this study, since it provides element-specific and momentum-dependent information for electronic excitations.<sup>10</sup> By tuning the incident photon energy to the Cu-K absorption edge, one can gain information concerning excitations localized around the Cu sites without suffering from problems due to the La bands. Furthermore, the momentum-resolving capability of RIXS provides additional information: the dispersion of such molecular orbital (MO) excitations. In this work, we find that  $\Delta_{\sigma\sigma^*}$  exhibits a strong, systematic dependence on the Cu-O bond length ( $d_{\text{Cu-O}}$ ), increasing as  $d_{\text{Cu-O}}$  is decreased. In addition, for materials with a small  $d_{\text{Cu-O}}$  and correspondingly large  $\Delta_{\sigma\sigma^*}$ , a relatively large dispersion of the MO excitation is observed. We discuss the implication of these observations for understanding the electronic structure of the cuprates.

## II. EXPERIMENTS

The RIXS experiments were carried out at the Advanced Photon Source on the undulator beamline 9IDB.

TABLE I: The copper oxide samples are listed along with the Cu-O bond lengths taken from the references. The top eight materials possess perfect square copper oxygen plaquettes, while the bottom three have distorted square plaquettes. Also listed are the polarization and the energy of the incident photon in RIXS measurements.

Label	Sample	Crystal <sup>a</sup>	$d_{\text{Cu-O}}$ (Å)	Ref. ( $d_{\text{Cu-O}}$ )	Polarization	$E_i$ (eV)	Ref. (RIXS)
2122	$\text{Sr}_2\text{CuO}_2\text{Cl}_2$	M	1.9858	12	$\epsilon \perp \mathbf{z}$	9001	This work
Nd	$\text{Nd}_2\text{CuO}_4$		1.9705	13	$\epsilon \perp \mathbf{z}$	8990	14
Ca	$\text{Ca}_2\text{CuO}_2\text{Cl}_2$		1.9344	15	$\epsilon \parallel \sim \mathbf{z}^b$	8996	16
2342	$\text{Sr}_2\text{Cu}_3\text{O}_4\text{Cl}_2$	M	1.929	17	$\epsilon \perp \mathbf{z}$	8998	This work
LCCO	$\text{La}_{1.9}\text{Ca}_{1.1}\text{Cu}_2\text{O}_6$	B	1.913	18	$\epsilon \parallel \mathbf{z}$	8999	This work
LCO	$\text{La}_2\text{CuO}_4$	T	1.904	19	$\epsilon \parallel \mathbf{z}$	8997	This work
LSCO5	$\text{La}_{1.95}\text{Sr}_{0.05}\text{CuO}_4$	C	1.898	19	$\epsilon \parallel \mathbf{z}$	8997	This work
LSCO17	$\text{La}_{1.83}\text{Sr}_{0.17}\text{CuO}_4$	C	1.885	19	$\epsilon \parallel \mathbf{z}$	8997	This work <sup>c</sup>
Li	$\text{Li}_2\text{CuO}_2$		1.9577	20	$\epsilon \perp \mathbf{z}$	8997	21
CGO	$\text{CuGeO}_3$		1.9326	22	$\epsilon \parallel \mathbf{x} + \mathbf{z}$	8990	23
112	$\text{SrCuO}_2$	U	1.910/1.930/1.961 <sup>d</sup>	24	$\epsilon \parallel \mathbf{z}$	8996	This work

<sup>a</sup>The crystals studied in this work were provided by various groups, which are denoted here as B:Brookhaven; C:CRIEPI; M:MIT; T:Toronto; U:Univ. of Tokyo.

<sup>b</sup>Since the polarization direction was in the scattering plane in this experiment, it changed as momentum transfer was varied.

<sup>c</sup>The RIXS data were taken at  $T = 15$  K.

<sup>d</sup> $\text{SrCuO}_2$  has three different copper-oxygen bond lengths, which are represented as large error bars in Fig. 2.

Experimental details have been described elsewhere.<sup>11</sup> Single crystal samples used in our measurements are listed in Table I, along with several samples studied in earlier RIXS experiments. In Table I,  $d_{\text{Cu-O}}$  and the experimental configuration is listed for each material. All measurements were performed at room temperature except for those on the LSCO17 sample. In our RIXS experiments, the scattering plane was vertical and the polarization of the incident x-ray,  $\epsilon$ , was perpendicular to the scattering plane. The polarization direction was kept fixed along the direction specified in Table I, where the coordinate system reference is the  $d_{x^2-y^2}$  orbital. That is, the copper oxygen plaquette lies in the  $xy$ -plane, while the  $z$ -direction is perpendicular to the plaquette. We use the notation of reduced momentum transfer  $\mathbf{q}$  throughout this paper, with the  $(\pi, 0)$  direction along the Cu-O bond direction.

Before discussing the experimental results in detail, it is useful to first review the second-order RIXS process to understand the nature of the observed excitation. In the ground state, the holes are located in the antibonding molecular orbital which is a combination of a Cu hole state ( $d^9$ ) and an oxygen ligand hole state ( $d^{10}\bar{L}$ ), with more weight on the  $d^9$  state. In the intermediate state of this resonance process, a Cu  $1s$  electron is excited to the Cu  $4p$  band, and the core hole potential alters the balance between the  $d^9$  and the  $d^{10}\bar{L}$  states. Then the lowest energy state is predominantly  $1sd^{10}\bar{L}4p$ , which is lower than  $1sd^94p$ . These states form the so-called well-screened and poorly-screened features, respectively, of the Cu K-edge x-ray absorption spectra (XAS). As discussed in detail by Hill and coworkers,<sup>9,25</sup> these intermediate states can decay into an excited state in which the hole in the antibonding molecular orbital is filled with an electron, cre-

ating a hole in the bonding orbital, and an energy loss in the outgoing photon. The RIXS process thus creates a charge-transfer excitation from bonding to antibonding molecular orbitals.

In our measurements, we have carefully studied the incident energy dependence in order to determine the resonance energy, for which the MO excitation has the maximum intensity. In most cases, the resonance energy, which is listed in Table I, corresponds to the higher energy peak (poorly-screened feature) in the XAS. On the other hand, the intensity of lower energy excitations near the charge transfer gap ( $\sim 2$  eV) is strongly enhanced when the incident energy corresponds to the well-screened intermediate state, as reported in earlier studies.<sup>11</sup> The resonance energy depends on the direction of the polarization vector. Detailed results of the incident energy dependence study will be published elsewhere. However, one should note that the energy-loss associated with the MO excitation does not depend on the incident polarization of the photon, although different  $4p$  states (e.g.,  $4p_\sigma$  or  $4p_\pi$ ) are involved in the intermediate state, as the polarization is varied with respect to the  $xy$ -plane.<sup>26</sup>

### III. RESULTS

In Fig. 1, representative RIXS scans are plotted. These are energy-loss scans taken at a fixed momentum transfer with the incident energy of the x-ray photon fixed at the values listed in Table I. The momentum transfer for all these scans has been fixed at  $\mathbf{q}=(\pi, 0)$ , which is the minimum energy position. The most striking feature in Fig. 1 is the large shift of the excitation energy from  $\sim 6$  eV for

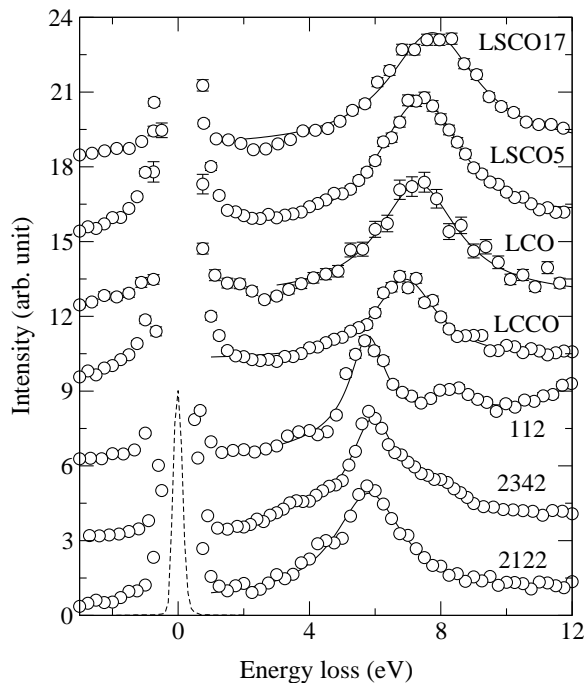


FIG. 1: RIXS spectra taken with the incident energy as specified in Table I for a fixed reduced wave vector of  $(\pi, 0)$ . Each spectrum is offset vertically for clarity, and solid lines are fits to a Lorentzian lineshape as described in the text. The dashed line is a representative scan through the elastic line, which shows instrumental energy resolution.

2122 to  $\sim 8$  eV for LSCO17. To analyze this shift quantitatively, we have fitted the observed excitation spectra to a simple Lorentzian lineshape and extracted the peak positions, which are plotted in Fig. 2(a) as a function of Cu-O bond length,  $d_{\text{Cu-O}}$ .

A few comments are in order regarding the data analysis. First, as is evident from the instrumental resolution plotted as a dashed line in Fig. 1, the observed excitations are not resolution-limited, hence justifying our simple fitting procedure, which does not convolve the data with the instrumental resolution. Second, in several cases, we observe more than one type of excitation in these scans. For example, the  $\text{SrCuO}_2$  data clearly shows a second feature around  $\sim 8.2$  eV, in addition to the main peak around  $\sim 6$  eV. In the 2342 case, there also seems to be two additional features, one at higher energy ( $\sim 8$  eV) and the other at lower energy ( $\sim 4$  eV). However, it is difficult to identify these weak features (if present) in the data for the other samples,<sup>27</sup> and we have chosen to fit all the scans with a single Lorentzian peak with a broad width. The peak positions extracted from our analysis are, therefore, those of the dominant features. In addition, the peak width extracted from the fits might in some cases arise from a distribution of several peaks over a wide energy range, rather than from a finite inverse lifetime of a single excitation. Finally, as discussed below, we observe dispersion of the MO excitation with momen-

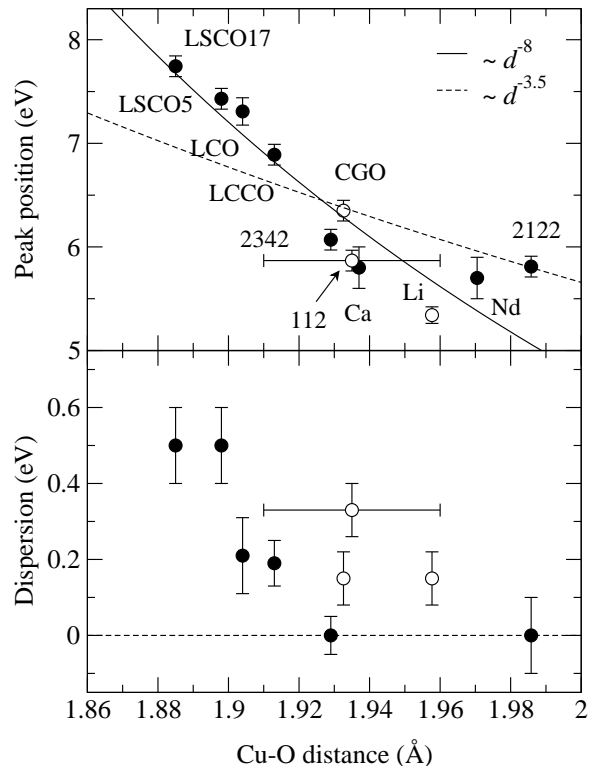


FIG. 2: (a) The value of the peak position at  $(\pi, 0)$ ,  $\Delta_{\sigma\sigma^*}$ , and (b) the amount of dispersion along the Cu-O bond direction for each sample is plotted as a function of  $d_{\text{Cu-O}}$ . The solid symbols are used for the perfect square plaquettes, while the open symbols are for the samples with distorted plaquettes. The solid and dashed lines are fits to power law expressions  $\Delta_{\sigma\sigma^*} \sim d_{\text{Cu-O}}^{-8}$  and  $d_{\text{Cu-O}}^{-3.5}$ , respectively. Note that the measured dispersion of the edge-sharing chain compounds Li and CGO is not along the Cu-O bond direction, while dispersion was not measured for Nd and Ca.<sup>9,16</sup>

tum transfer. This can be as large as  $\sim 0.5$  eV in some of the compounds studied, as shown in Fig. 3. Thus, the peak position of the MO excitation depends not only on the sample, but also on  $\mathbf{q}$ . The scans shown in Fig. 1 all are taken at the minimum energy position,  $\mathbf{q} = (\pi, 0)$ , and the peak positions plotted in Fig. 2(a) are the values measured at this position.

As shown in Fig. 2(a), the energy of the MO excitation exhibits a strong dependence on  $d_{\text{Cu-O}}$ . It is noteworthy that the excitation energy exhibits such a systematic dependence on the *local* structure, and that it is apparently insensitive to whether the crystal has a planar, corner-sharing, or edge-sharing chain structure. This is consistent with our assignment of these features as MO excitations localized within a single Cu-O plaquette.

The overall trend exhibited in Fig. 2(a) is not unexpected. Intuitively, as the Cu and O atoms move closer, the  $p-d$  overlap will increase, and the Cu-O bonding becomes more covalent with a larger energy splitting  $\Delta_{\sigma\sigma^*}$ . What is surprising is how strong this

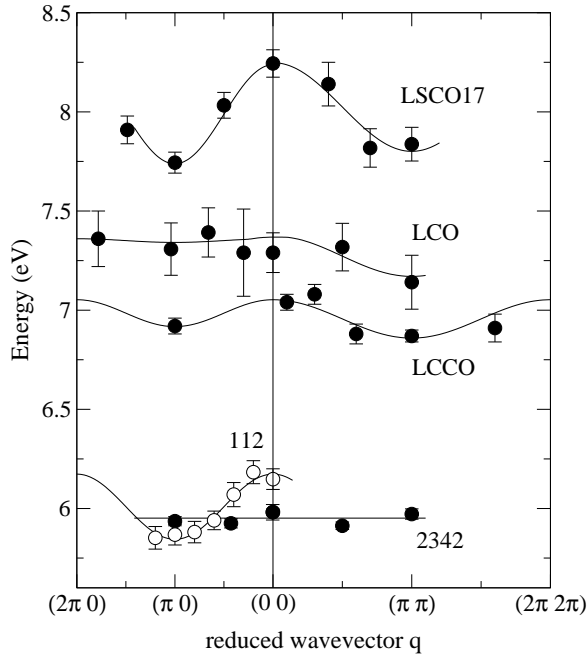


FIG. 3: The observed dispersion of the MO excitation. The left panel is along the  $(\pi 0)$  direction, and the right panel is data taken along the  $(\pi \pi)$  direction. The solid lines are guides to the eye.

$d_{\text{Cu-O}}$  dependence is. We have modeled the  $d_{\text{Cu-O}}$ -dependence of  $\Delta_{\sigma\sigma^*}$  as a power law ( $\Delta_{\sigma\sigma^*} \sim d^\eta$ ) and find  $\eta = -8(2)$ , shown as a solid line in Fig. 2(a). Note that the MO excitation energy is expected to be given by<sup>2</sup>  $\Delta_{\sigma\sigma^*} = \sqrt{(2t_{pp} - \Delta_0)^2 + 16t_{pd}^2}$ , where  $t_{pp} \approx 0.65$  eV is the hopping matrix element between the oxygen  $p$  orbitals.<sup>1</sup> Since  $16t_{pd}^2 \gg (2t_{pp} - \Delta_0)^2$ , this expression leads to  $\Delta_{\sigma\sigma^*} \approx 4t_{pd}$ , to a first approximation, and one then expects similar a  $d$ -dependence for  $\Delta_{\sigma\sigma^*}$  and  $t_{pd}$ . Our results then implies that the  $d$ -dependence of  $t_{pd}$  is much stronger than that expected from tight-binding theory, for which  $\sim d^{-3.5}$  is predicted.<sup>28</sup> As plotted in Fig. 2(a), the observed RIXS data clearly deviates from the  $\Delta_{\sigma\sigma^*} \sim d^{-3.5}$  behavior (dashed line). We also note that the  $t_{pd} \sim d^{-8}$  behavior determined from our RIXS measurements is different from the earlier report of  $t_{pd} \sim d^{-4}$  by Cooper and coworkers, which was estimated indirectly from a three-band Hubbard model expression.<sup>29</sup>

In Fig. 3, the dispersion of the MO excitation is plotted as a function of  $\mathbf{q}$  for selected samples. These data suggest that the picture of a completely localized MO excitation is an oversimplification – such a model would predict no dispersion of these features. The data of Fig. 2(b), which show significant dispersion for  $d_{\text{Cu-O}} < 1.93$  Å, suggest then that this localized picture breaks down for small bond distances. For the LSCO17 sample, the dispersion bandwidth is about 0.5 eV, with the minimum excitation energy occurring at the zone boundary, imply-

ing an indirect gap. Note that this is completely different from the direct nature of the lower energy charge-transfer gap as reported in Ref. 11. As  $\Delta_{\sigma\sigma^*}$  decreases (e.g., LCO and LCCO), the dispersion of the MO excitation becomes weaker. For the samples with an even smaller  $\Delta_{\sigma\sigma^*}$ , the dispersion becomes flat, as shown for the 2342 sample (Figs. 2 and 3). Limited momentum dependence measurements for the 2122 sample (not shown) also show a dispersionless behavior. The size of the observed dispersion along the Cu-O bond direction is plotted against  $d_{\text{Cu-O}}$  in Fig. 2(b).

As shown in Fig. 2, the size of the dispersion and  $\Delta_{\sigma\sigma^*}$  both increase as  $d_{\text{Cu-O}}$  decreases. This suggests that the bandwidth of the dispersion is also controlled by the hopping parameter  $t_{pd}$ . Such behavior would, of course, be expected from the increased overlap of the wavefunctions, since charge carriers then become less localized. However, the simplest picture of delocalized electrons fails to describe the observed dispersion. For example, the bandwidths of the Cu-O bonding and antibonding bands in LCO are very large  $\sim 3$  eV, and interband transitions between these two bands would have a *direct* gap of  $\sim 4$  eV.<sup>3,4</sup>

#### IV. DISCUSSION AND SUMMARY

One of the most surprising results in this study is that the  $\Delta_{\sigma\sigma^*} - d_{\text{Cu-O}}$  scaling seems to apply to different structures. In contrast, previous studies of the bond-length scaling of various quantities, such as charge-transfer gap ( $\Delta_{CT}$ ), or superexchange interaction ( $J$ ), have been limited to compounds with corner-sharing structures.<sup>30</sup> It is well known that such quantities as superexchange coupling depend not only on the  $p - d$  hybridization, but also crucially on the angle between the two Cu-O bonds.<sup>32</sup> One can argue that  $\Delta_{\sigma\sigma^*}$  is a better measure of Cu-O hybridization than  $J$  or  $\Delta_{CT}$ , since it is only dependent on  $d_{\text{Cu-O}}$  and not on the presence of neighboring atoms.

We have noted that the  $t_{pd} \sim d^{-8}$  dependence inferred from our study deviates significantly from the tight-binding picture. It also appears to give rise to discrepancies with other experiments. For example, for materials with the corner-sharing structure, the three-band Hubbard model gives  $J \sim t_{pd}^4 / U^* \Delta_{CT}^2$ , where  $U^*$  is an effective onsite Coulomb interaction which is assumed to be constant. If we use the experimentally determined<sup>29</sup>  $\Delta_{CT} \sim d^{-6}$  and our  $t_{pd} \sim d^{-8}$  result, we obtain  $J \sim d^{-20}$ , which clearly disagrees with the much weaker  $d$ -dependence of  $J$  observed in various experiments, including two magnon Raman scattering.<sup>31</sup> One might expect that this discrepancy could be resolved by considering the fact that, due to strong electron correlations, the simple tight-binding picture of covalent bonding has to be modified. In fact, Mizuno and coworkers<sup>33</sup> considered two contributions to  $t_{pd}$ . That is,  $t_{pd} = t_{pd}^0 + t_{pd}^M$ , where  $t_{pd}^0$  is the contribution from the

atomic potential which depends only on  $d_{\text{Cu-O}}$ , while  $t_{pd}^M$  is the contribution from the Madelung potential, which depends on the detailed arrangement of the neighboring ions. However, the calculated contribution from the Madelung potential is of order of  $\sim 0.1$  eV or smaller,<sup>33</sup> so that this alone is not enough to explain the  $\sim d^{-8}$  dependence.

These results may be suggesting that one has to abandon the simple relationship of  $\Delta_{\sigma\sigma^*} \approx 4t_{pd}$ . Certainly, as discussed above, the picture of a completely localized MO excitation is apparently an oversimplification, since it breaks down as  $d_{\text{Cu-O}}$  becomes shorter – as evidenced by the sizable dispersion observed in LSCO17. Thus, if a more realistic expression for  $\Delta_{\sigma\sigma^*}$  is used,  $t_{pd} \sim d^{-3.5}$  scaling law might be recovered. For example, a recent first-principles calculation has emphasized the role of apical oxygens in the systematics of high temperature superconductivity<sup>34</sup>. Indeed, the scaling plot in Fig. 2 also exhibits some systematic dependence on the number of apical oxygens,<sup>35</sup> and it may be interesting to further investigate the role played by apical oxygens. Certainly, a systematic *ab initio* calculation of the  $d_{\text{Cu-O}}$ -dependence of MO excitation energy in large clusters would be highly desirable and may help to clarify the relationship between  $\Delta_{\sigma\sigma^*}$ ,  $t_{pd}$ , and  $d_{\text{Cu-O}}$ .

To summarize, we have studied a charge-transfer exci-

tation in various cuprate compounds using resonant inelastic x-ray scattering technique. We assign this excitation to a mostly localized molecular orbital excitation, that is, an excitation from a bonding to an antibonding molecular orbital. We have found that this molecular orbital excitation energy, which is a measure of the hopping matrix element  $t_{pd}$ , exhibits a systematic Cu-O bond length dependence, which is much stronger than that expected from tight-binding theory. We have also observed a sizable dispersion of this excitation in some materials, suggesting that this molecular orbital excitation becomes less localized as the  $p-d$  hybridization becomes large.

### Acknowledgments

We would like to thank P. D. Johnson, G. A. Sawatzky, and M. A. van Veenendaal for invaluable discussions. The work at Brookhaven was supported by the U. S. Department of Energy, Division of Materials Science, under contract No. DE-AC02-98CH10886. Use of the Advanced Photon Source was supported by the U. S. Department of Energy, Basic Energy Sciences, Office of Science, under Contract No. W-31-109-Eng-38.

- 
- <sup>1</sup> M. S. Hybersten, M. Schlüter, and N. E. Christensen, Phys. Rev. B **39**, 9028 (1989).
  - <sup>2</sup> M. A. van Veenendaal, H. Eskes, and G. A. Sawatzky, Phys. Rev. B **47**, 11462 (1993).
  - <sup>3</sup> L. F. Mattheiss, Phys. Rev. Lett. **58**, 1028 (1987).
  - <sup>4</sup> A. K. McMahan, R. M. Martin, and S. Satpathy, Phys. Rev. B **38**, 6650 (1988).
  - <sup>5</sup> R. L. Martin and P. J. Hay, J. Chem. Phys. **98**, 8680 (1993).
  - <sup>6</sup> P. Hüsler, H. U. Suter, E. P. Stoll, and P. F. Meier, Phys. Rev. B **61**, 1567 (2000).
  - <sup>7</sup> S. Uchida, T. Ido, H. Takagi, T. Arima, Y. Tokura, and S. Tajima, Phys. Rev. B **43**, 7942 (1991).
  - <sup>8</sup> C. C. Kao, W. A. L. Caliebe, J. B. Hastings, and J. M. Gillet, Phys. Rev. B **54**, 16361 (1996).
  - <sup>9</sup> J. P. Hill, C. C. Kao, W. A. L. Caliebe, M. Matsubara, A. Kotani, J. L. Peng, and R. L. Greene, Phys. Rev. Lett. **80**, 4967 (1998).
  - <sup>10</sup> A. Kotani and S. Shin, Rev. Mod. Phys. **73**, 203 (2001).
  - <sup>11</sup> Y. J. Kim, J. P. Hill, C. A. Burns, S. Wakimoto, R. J. Birgeneau, D. Casa, T. Gog, and C. T. Venkataraman, Phys. Rev. Lett. **89**, 177003 (2002).
  - <sup>12</sup> L. L. Miller, X. L. Wang, S. X. Wang, C. Stassis, D. C. Johnston, J. Faber, Jr., and C.-K. Loong, Phys. Rev. B **41**, 1921 (1990).
  - <sup>13</sup> J. Gopalakrishnan, M. A. Subramanian, C. C. Torardi, J. P. Attfield, and A. W. Sleight, Mater. Res. Bull. **24**, 321 (1989).
  - <sup>14</sup> J. P. Hill, C. C. Kao, M. v. Zimmermann, K. Hämmäläinen, S. Huotari, L. E. Berman, W. A. L. Caliebe, K. Hirota, M. Matsubara, A. Kotani, J. L. Peng, R. L. Greene, I. T. dn T Masuda, and K. Uchinokura, Jpn. J. Appl. Phys. **38**, 118 (1999).
  - <sup>15</sup> D. N. Argyriou, J. D. Jorgensen, R. L. Hitterman, Z. Hiroi, N. Kobayashi, and M. Takano, Phys. Rev. B **51**, 8434 (1995).
  - <sup>16</sup> M. Z. Hasan, E. D. Isaacs, Z. X. Shen, L. L. Miller, K. Tsutsui, T. Tohyama, and S. Maekawa, Science **288**, 1811 (2000).
  - <sup>17</sup> Y. J. Kim, R. J. Birgeneau, F. C. Chou, M. Greven, M. A. Kastner, Y. S. Lee, B. O. Wells, A. Aharony, O. Entin-Wohlman, I. Y. Korenblit, A. B. Harris, R. W. Erwin, and G. Shirane, Phys. Rev. B **64**, 024435 (2001).
  - <sup>18</sup> F. Izumi, E. Takayama-muromachi, Y. Nakai, and H. Asano, Physica C **157**, 89 (1989).
  - <sup>19</sup> P. G. Radaelli, D. G. Hinks, A. W. Mitchell, B. A. Hunter, J. L. Wagner, B. Dabrowski, K. G. Vandervoort, H. K. Viswanathan, and J. D. Jorgensen, Phys. Rev. B **49**, 4163 (1994).
  - <sup>20</sup> F. Sapina, J. Rodriguez-Carvajal, M. J. Sanchis, R. Ibanes, A. Beltran, and D. Beltran, Solid State Commun. **74**, 779 (1990).
  - <sup>21</sup> Y. J. Kim, J. P. Hill, F. C. Chou, D. Casa, T. Gog, and C. T. Venkataraman, Phys. Rev. B **69**, 155105 (2004).
  - <sup>22</sup> M. Braden, G. Wilkendorf, J. Lorenzana, M. Ain, G. J. McIntyre, M. Behruzi, G. Heger, G. Dhalenne, and A. Revcolevschi, Phys. Rev. B **54**, 1105 (1996).
  - <sup>23</sup> M. v. Zimmermann, J. P. Hill, C. C. Kao, T. Ruf, T. Gog, C. Venkataraman, I. Tsukada, and K. Uchinokura, unpublished (2001).
  - <sup>24</sup> Y. Matsushita, Y. Oyama, M. Hasegawa, and H. Takei, J. Solid State Chem. **114**, 289 (1994).

- <sup>25</sup> T. Ide and A. Kotani, J. Phys. Soc. Japan **68**, 3100 (1999); *ibid.* **69**, 3107 (2000).
- <sup>26</sup> K. Hämäläinen, J. P. Hill, S. Huotari, C. C. Kao, L. E. Berman, A. Kotani, T. Idé, J. L. Peng, and R. L. Greene, Phys. Rev. B **61**, 1836 (2000).
- <sup>27</sup> A possible origin of the lack of multiple-peak structure in some samples might be the polarization dependent selection rule, which forbid excitations of certain symmetries. (See P. Abbamonte *et al.*, cond-mat/9911215)
- <sup>28</sup> W. A. Harrison, *Electronic Structure and the Properties of Solids* (Dover, New York, 1989).
- <sup>29</sup> S. L. Cooper, G. A. Thomas, A. J. Millis, P. E. Sulewski, J. Orenstein, D. H. Rapkine, S. W. Cheong, and P. L. Trevor, Phys. Rev. B **42**, 10785 (1990).
- <sup>30</sup> Y. Ohta, T. Tohyama, and S. Maekawa, Phys. Rev. Lett. **66**, 1228 (1991).
- <sup>31</sup> P. E. Sulewski, P. A. Fleury, K. B. Lyons, S.-W. Cheong, and Z. Fisk, Phys. Rev. B **41**, 225 (1990).
- <sup>32</sup> Y. Mizuno, T. Tohyama, S. Maekawa, T. Osafune, N. Motoyama, H. Eisaki, and S. Uchida, Phys. Rev. B **57**, 5326 (1998).
- <sup>33</sup> Y. Mizuno, T. Tohyama, and S. Maekawa, Phys. Rev. B **58**, R14713 (1998).
- <sup>34</sup> E. Pavarini, I. Dasgupta, T. Saha-Dasgupta, O. Jepsen, and O. K. Andersen, Phys. Rev. Lett. **87**, 047003 (2001).
- <sup>35</sup> There are two apical oxygens in the structure of LSCO17, LSCO5, and LCO, while there is one apical oxygen for LCCO. The rest of the samples have no apical oxygens.